Electronic Supporting Information

$Ni_{12}P_5$ Nanoparticles Decorated on Carbon Nanotubes with Enhanced Electrocatalytic and Lithium Storage Properties

Chunde Wang, Tao Ding, Yuan Sun, Xiaoli Zhou, Yun Liu, Qing Yang*

Hefei National Laboratory of Physical Sciences at the Microscale (HFNL), Department of Chemistry, Laboratory of Nanomaterials for Energy Conversion (LNEC) and Synergetic Innovation Center of Quantum Information & Quantum Physics, University of Science and Technology of China (USTC), Hefei, Anhui 230026, The People's Republic of China

* E-mail: qyoung@ustc.edu.cn; Fax: +86-551-63606266; Tel: +86-551-63600243

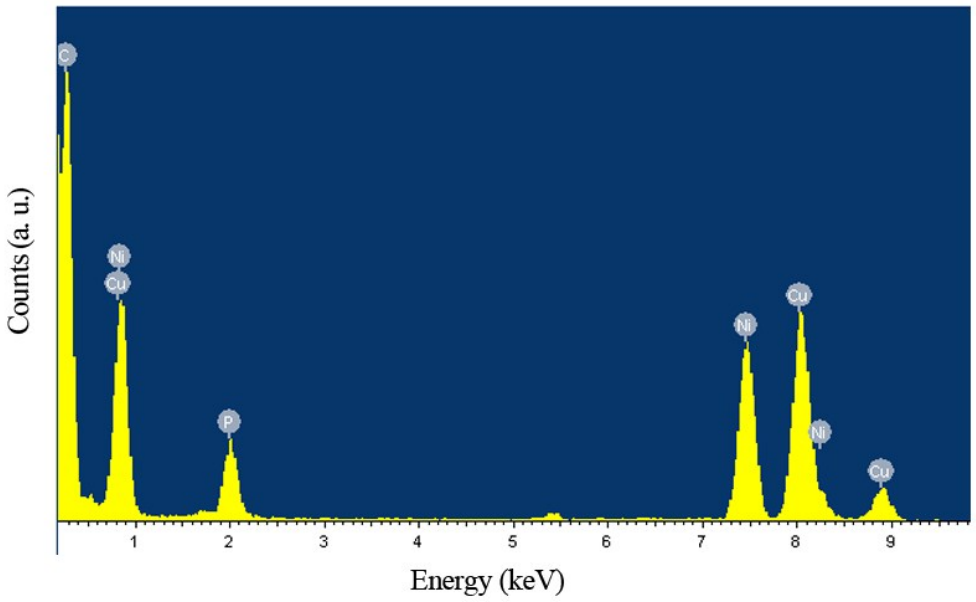

Figure S1. EDX spectrum of the as-synthesized monodisperse $Ni_{12}P_5$ nanoparticles. The signal of Cu and C arises from the TEM grid made of Cu.

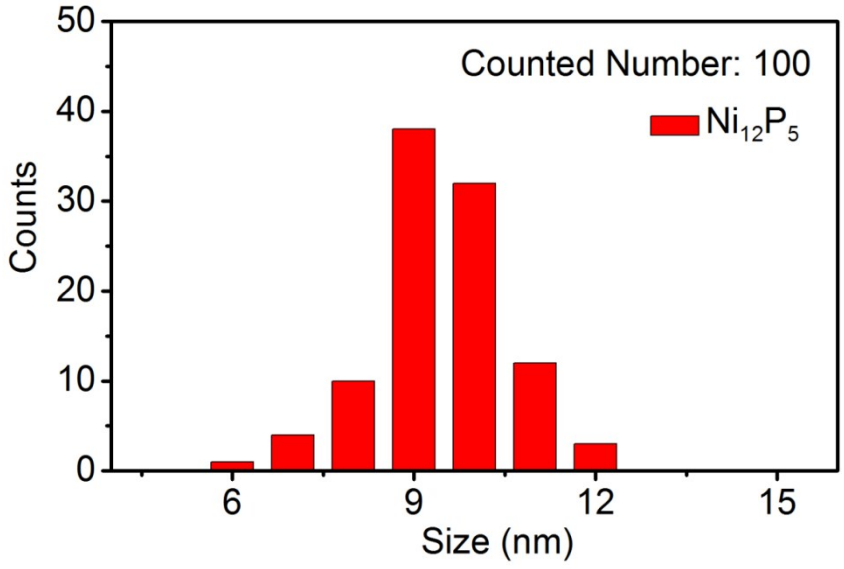

Figure S2. Statistic histogram of size distribution for the $Ni_{12}P_5$ nanoparticles. The data are obtained based on manual counts of 100 nanoparticles from TEM images.

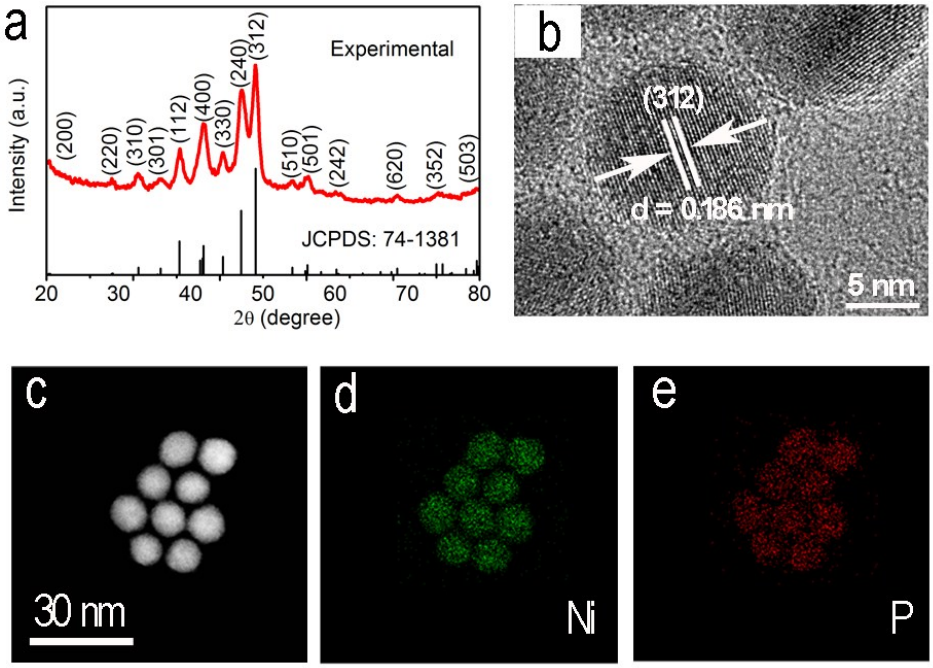

Figure S3. (a) XRD patterns, and (b) corresponding HRTEM images of the monodisperse $Ni_{12}P_5$ nanoparticles, and (c-e) corresponding EDX maps of the elements of Ni and P.

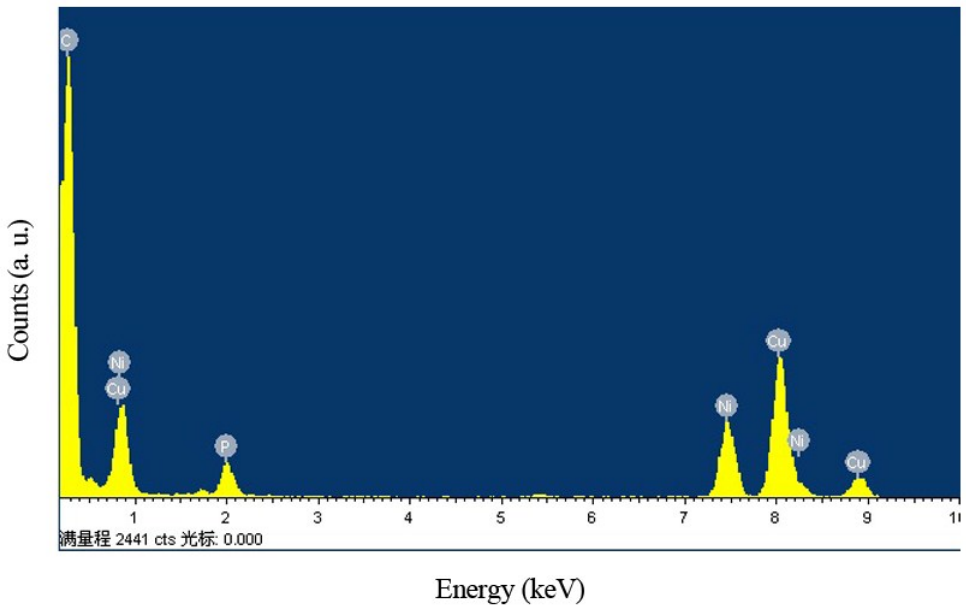

Figure S4. EDX spectrum of the $Ni_{12}P_5$/CNT nanohybrids.

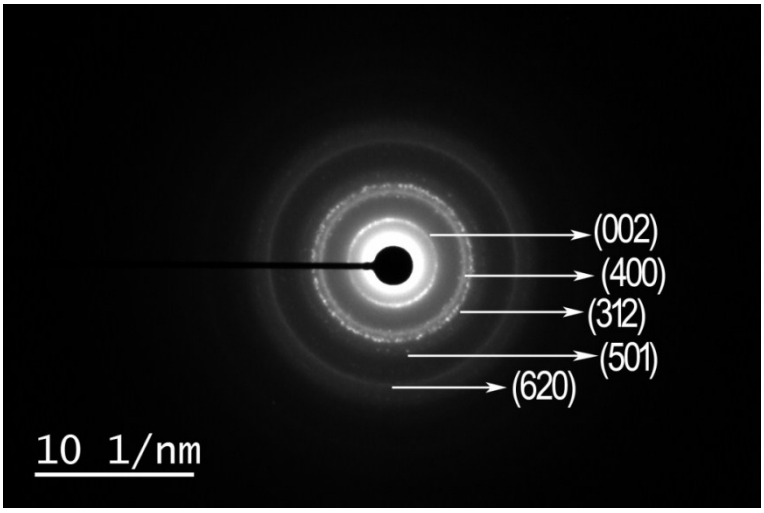

Figure S5. An electron diffraction pattern of the $Ni_{12}P_5$/CNT nanohybrids.

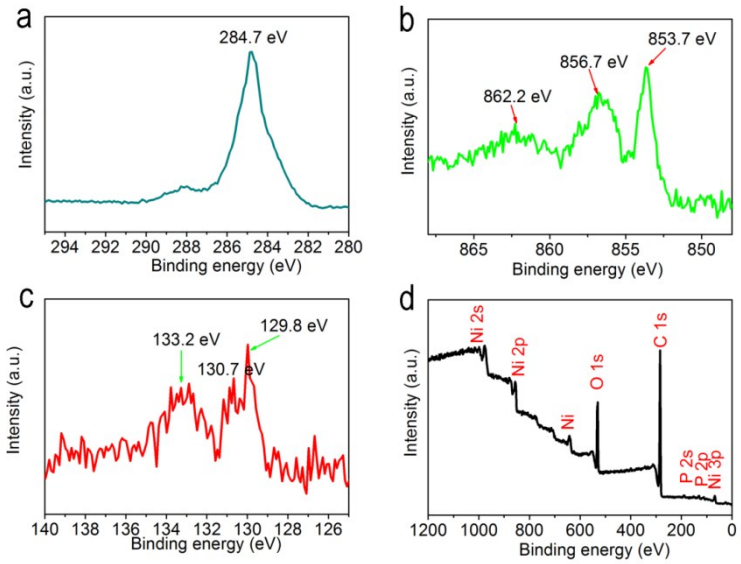

Figure S6. XPS spectra of (a) C 1s, (b) Ni 2p, (c) P 2p and (d) survey spectrum regions for the $Ni_{12}P_5$/CNT nanohybrids.

Table S1. Comparison of HER performance in acidic media for $Ni_{12}P_5$/CNT with other non-noble metal HER electrocatalysts.

Catalyst	Current density (j, mA/cm^2)	Overpotential at the corresponding j (mV)	Reference
CoP/CNT	10	122	Angew. Chem. Int. Ed. 2014, 53, 6710
Amorphous WP nanoparticles	10	120	Chem. Commun. 2014, 50, 11026
	20	140	
FeP	10	~240	Chem. Commun. 2013, 49, 6656
CoP/Ti	10	90	Chem. Mater. 2014, 26, 4326
	100	146	
MoS_2/Graphene/CP	10	150	J. Am. Chem. Soc. 2011, 133, 7296
Ni_2P /CNT	10	124	J. Mater. Chem. A 2015, 3 , 13087
MoS_2/graphene/Ni foam	10	141	Adv. Mater. 2013, 25, 756
	100	263	
MoS_2/MoO_3 /FTO	10	300	Nano Lett. 2011, 11, 4168
MoP nanoparticles	2	84	Adv. Mater. 2014, 26, 5702
	10	125	
	100	200	
Ni_2P hollow nanoparticles/Ti	10	116	J. Am. Chem. Soc. 2013, 135, 9267
	100	180	
Amorphous MoP Nanoparticles	10	90	Chem. Mater. 2014, 26, 4826
Cu_3P NW/CF	1	79	Angew. Chem. Int. Ed. 2014, 53, 9577
	10	143	
	100	276	
$Ni_{12}P_5$/CNT	2	65	This work
	10	129	

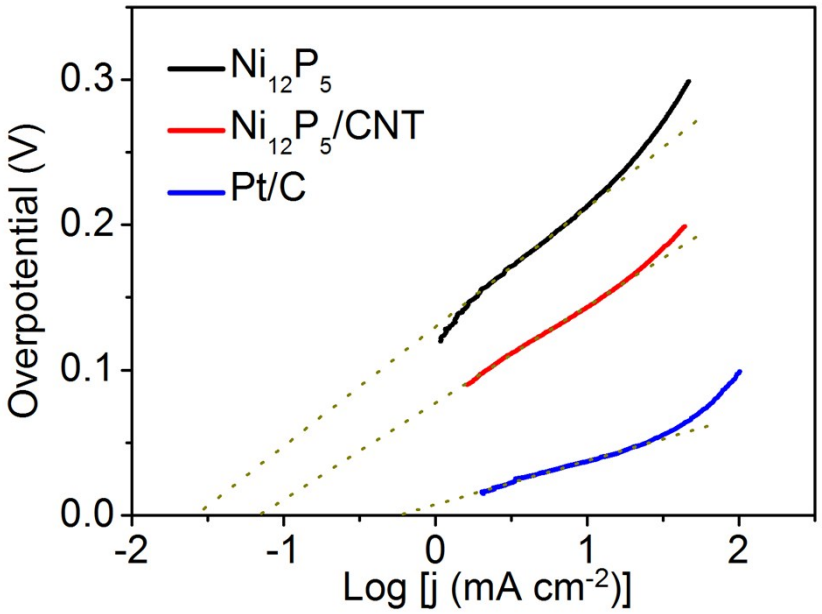

Figure S7. Calculation of the exchange current density of $Ni_{12}P_5$, $Ni_{12}P_5$/CNT and Pt/C by extrapolation method.

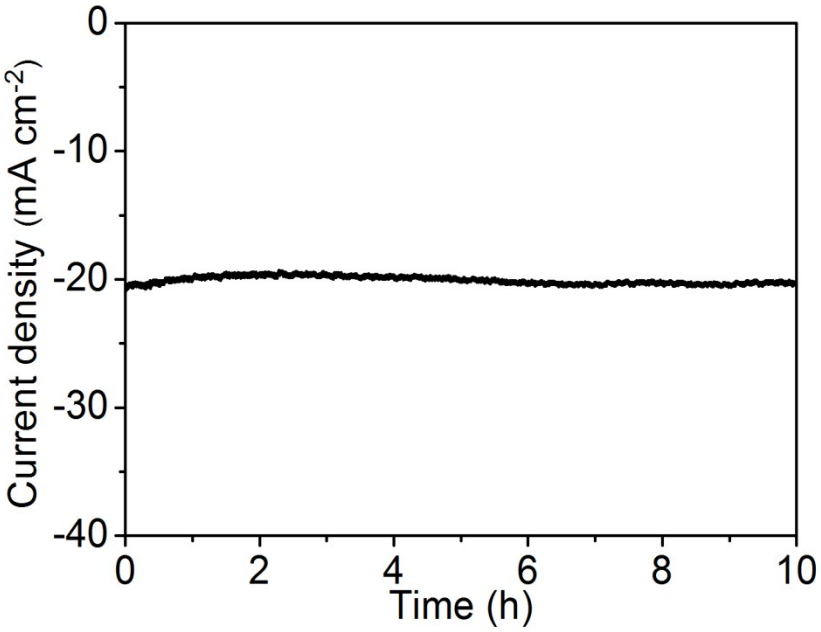

Figure S8. Time dependence of the current density under a constant overpotential of 160 mV of $Ni_{12}P_5$/CNT.

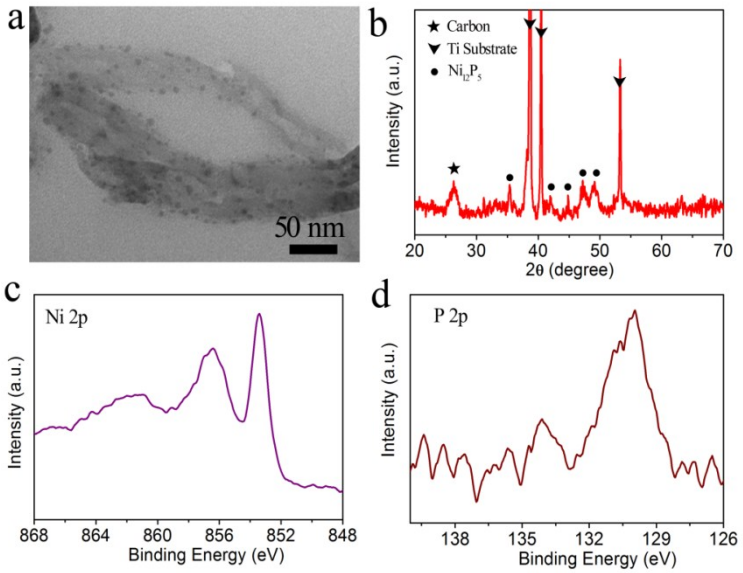

Figure S9. TEM image, XRD pattern and XPS spectra of $Ni_{12}P_5$/CNT catalysts after 1000 cycling.

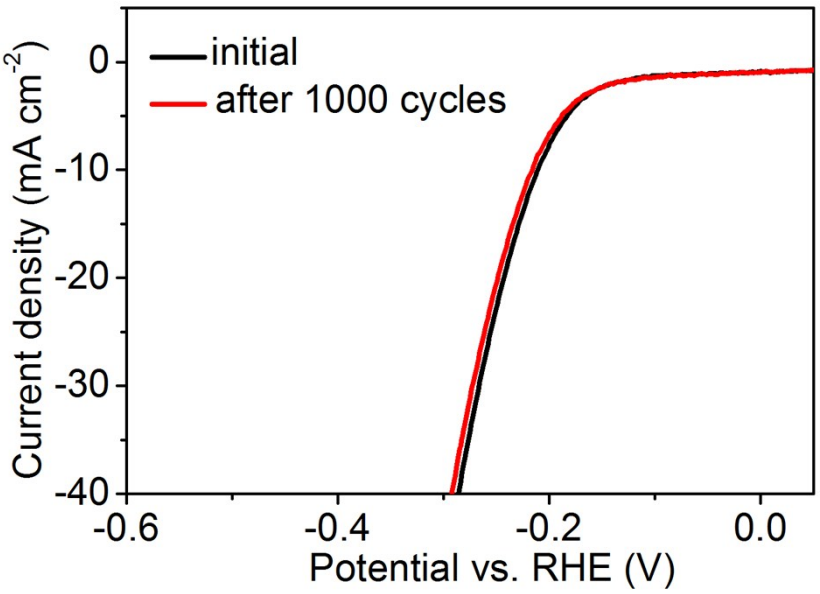

Figure S10. Polarization curves for $Ni_{12}P_5$ in H_2SO_4 solution (0.5 M) with a scan rate of 5 mV s^{-1} before and after 1000 cycles.

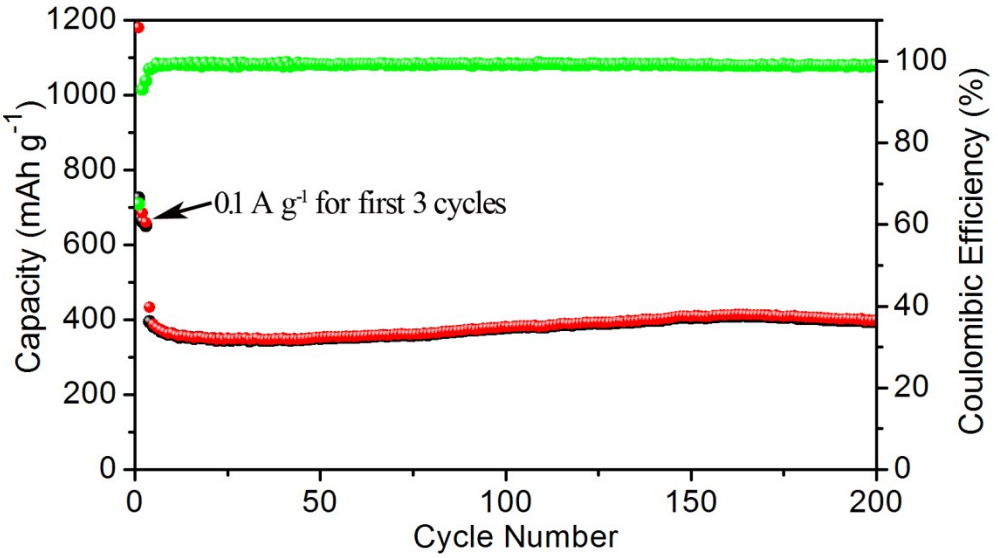

Figure S11. Cycling performance and the corresponding Coulombic efficiency of the annealed $Ni_{12}P_5$/CNT nanohybrids at a current density of 2.0 A g^{-1}.

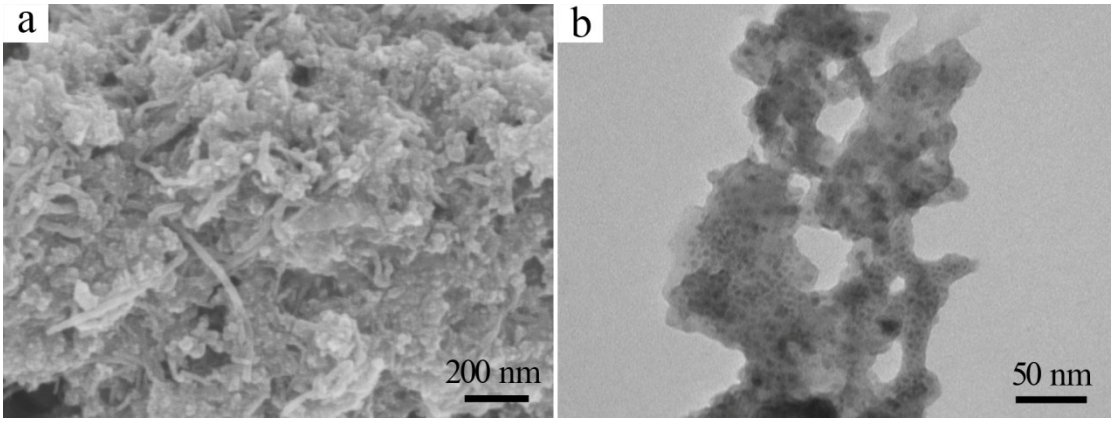

Figure S12. SEM (a) and TEM (b) images of the $Ni_{12}P_5$/CNT nanohybrids electrodes after 100 cycles at 100 mA g^{-1}.

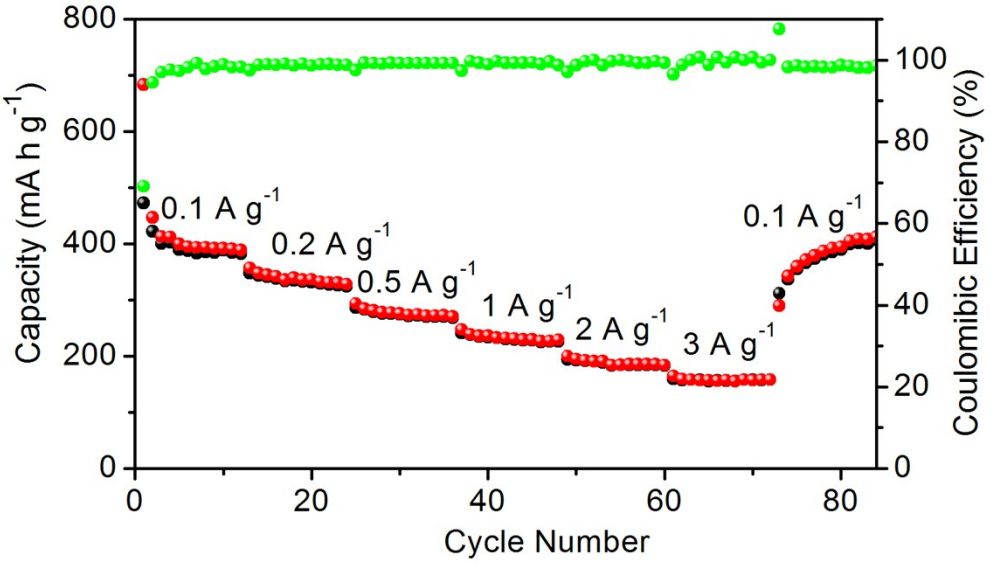

Figure S13. Rate performance and the corresponding Coulombic efficiency of the annealed bare $Ni_{12}P_5$ nanoparticles.

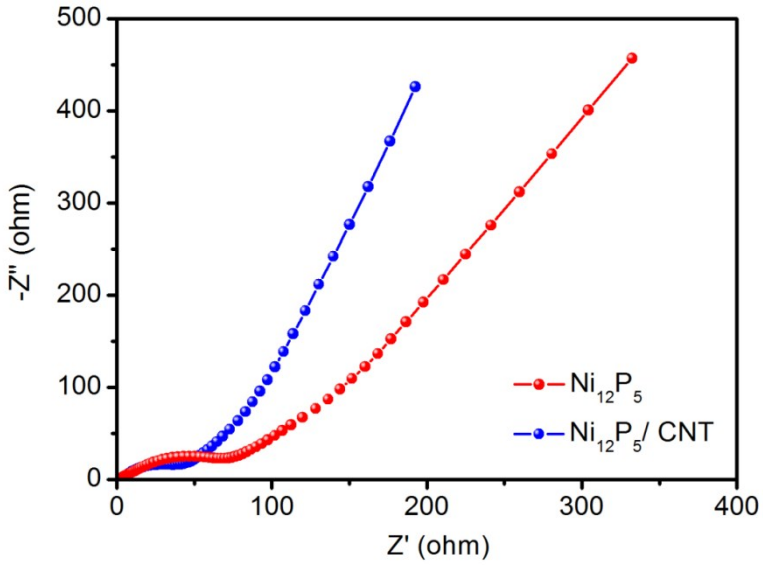

Figure S14. Nyquist plots of the annealed $Ni_{12}P_5$/CNT nanohybrids and the annealed bare $Ni_{12}P_5$ nanoparticles.

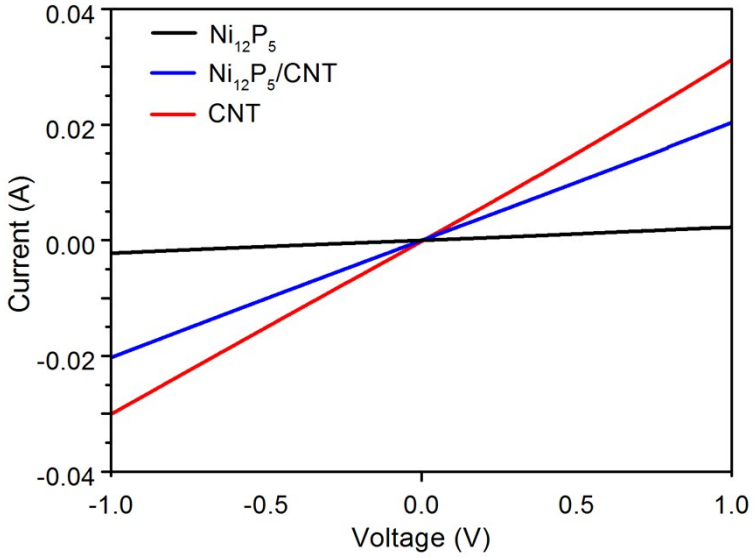

Figure S15. Typical I–V curves measured of the different samples at room temperature.